Cell Reports

Report

Wnt signaling inhibits casein kinase 1α activity by modulating its interaction with protein phosphatase 2A

Graphical abstract

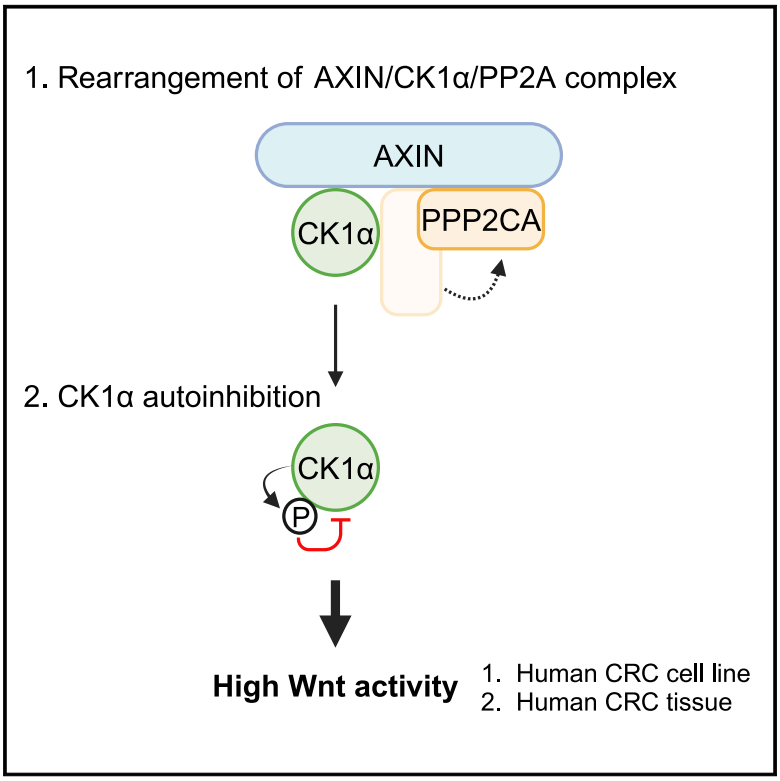

Highlights

- Wnt signaling induces CK1α autophosphorylation, which inhibits CK1α activity
- Wnt signaling regulates the dynamics of CK1α/PP2A/AXIN complex, causing CK1α autoinhibition
- Autophosphorylated CK1α is enriched in a subset of Wnt-dependent colorectal cancers

Authors

Chen Shen, Wenhui Lu, Siva B. Merugu, ..., Ethan Lee, Yashi Ahmed, David J. Robbins

Correspondence

dr956@georgetown.edu

In brief

Shen et al. show that the activity of a ubiquitous enzyme, CK1α, is autoinhibited upon the stimulation of Wnt signaling. The underlying mechanism involves the rearrangement of a multiprotein complex consisting of CK1α, PP2A, and AXIN. The authors further illustrate the importance of CK1α autoinhibition in colorectal cancer growth.

Shen et al., 2025, Cell Reports *44*, 115274
February 25, 2025
https://doi.org/10.1016/j.celrep.2025.115274

CellPress

Cell Reports

CellPress
OPEN ACCESS

Report

Wnt signaling inhibits casein kinase 1α activity by modulating its interaction with protein phosphatase 2A

Chen Shen,[1,8] Wenhui Lu,[1,8] Siva B. Merugu,[1,8] Aradhana Bharti,[1] Said M. Afify,[1] Lauren Schnitkey,[2] Daniel T. Wynn,[1] Fan Yang,[1] Thomas M. Rohwetter,[1] Anmada Nayak,[1] Nawat Bunnag,[3] Carolina Cywiak,[2] Hsin-Yao Tang,[4] Brent T. Harris,[1] Christopher Albanese,[1,5] Chukwuemeka Ihemelandu,[6] Melanie H. Cobb,[7] Arminja Kettenbach,[3] Ethan Lee,[2] Yashi Ahmed,[3] and David J. Robbins[1,9,*]

[1]Department of Oncology, Lombardi Comprehensive Cancer Center, Georgetown University, Washington, DC 20057, USA
[2]Department of Cell and Developmental Biology, Vanderbilt University, Nashville, TN 37232, USA
[3]Department of Molecular and Systems Biology and the Dartmouth Cancer Center, Geisel School of Medicine, Dartmouth College, Hanover, NH 03755, USA
[4]Molecular and Cellular Oncogenesis Program, The Wistar Institute, Philadelphia, PA 19104, USA
[5]Department of Radiology, Lombardi Comprehensive Cancer Center, Georgetown University, Washington, DC 20057, USA
[6]Department of Surgical Oncology, Lombardi Comprehensive Cancer Center, Georgetown University, Washington, DC 20057, USA
[7]Department of Pharmacology, University of Texas Southwestern Medical Center, Dallas, TX 75390, USA
[8]These authors contributed equally
[9]Lead contact
*Correspondence: dr956@georgetown.edu
https://doi.org/10.1016/j.celrep.2025.115274

SUMMARY

The mechanism by which Wnt signaling, an essential pathway controlling development and disease, stabilizes β-catenin has been a subject of debate over the last four decades. Casein kinase 1α (CK1α) functions as a pivotal negative regulator of this signaling pathway, initiating the events that destabilize β-catenin. However, whether and how CK1α activity is regulated in Wnt-off and Wnt-on states remains poorly understood. We now show that CK1α activity requires its association with the α catalytic subunit of protein phosphatase 2A (PPP2CA) on AXIN, the scaffold protein of the β-catenin destruction complex. Wnt stimulation induces the dissociation of PPP2CA from CK1α, resulting in CK1α autophosphorylation and its consequent inactivation. Moreover, autophosphorylated CK1α is enriched in a subset of colorectal cancers (CRCs) harboring constitutive Wnt activation. Our findings identify a mechanism by which Wnt stimulation inactivates CK1α, filling a critical gap in our understanding of Wnt signaling, with relevance for CRC.

INTRODUCTION

Wnt signaling is an evolutionarily conserved signal transduction cascade that regulates diverse cellular processes in both development and disease.[1,2] In the absence of Wnt ligands, the β-catenin destruction complex, consisting of AXIN, adenomatous polyposis coli (APC), glycogen synthase kinase 3 (GSK3), and casein kinase 1α (CK1α), induces the phosphorylation-dependent degradation of the Wnt signaling effector β-catenin.[3–8] Within this complex, CK1α initiates the process of β-catenin degradation via its phosphorylation on S45, consistent with its function as a crucial negative regulator of Wnt signaling.[7–9] Recently, CK1α activation by small-molecule activators has been reported to inhibit the onset and progression of Wnt-driven diseases, such as colorectal cancer (CRC), the vast majority of which acquire constitutive Wnt activation via mutations in the β-catenin destruction complex.[9–11] A small-molecule CK1α agonist attenuated tumor growth in a CRC mouse model but, surprisingly, did not disturb normal Wnt-regulated intestinal homeostasis.[11] Thus, in contrast with other Wnt inhibitors that target CRCs with destruction complex mutations, CK1α agonists overcome a major hurdle, which is the on-target disruption of normal intestinal homeostasis.[11] These results also highlighted the regulation of CK1α in physiological and pathological settings as an important gap in our understanding of Wnt signaling.

Unlike other CK1 family members,[12–16] CK1α was initially proposed to function as a constitutively active protein kinase in the Wnt signaling pathway.[8] However, other studies suggested that the CK1α-mediated phosphorylation of β-catenin might be regulated by Wnt stimulation,[7,17] although the mechanism was not determined. In the current study, we now show that the catalytic activity of CK1α is indeed modulated in response to Wnt ligands. Furthermore, we show that Wnt-mediated CK1α inhibition occurs via disruption of its association with protein phosphatase 2A (PP2A); CK1α consequently undergoes autophosphorylation and inactivation of its catalytic activity. Finally, we provide evidence that this mechanism of CK1α regulation may be relevant for a subset of CRCs.

RESULTS

Wnt signaling regulates CK1α kinase activity

To determine whether Wnt signaling regulates the catalytic activity of CK1α, we isolated endogenous CK1α from 293T cells treated with recombinant Wnt3a and used the phosphorylation of β-catenin S45, a CK1α-specific substrate, as a readout for CK1α activity.[7,8] CK1α isolated in this manner phosphorylated recombinant β-catenin at S45, and this kinase activity was significantly inhibited by Wnt3a treatment (Figures 1A, 1B, and S1A). Post-translational modifications, particularly phosphorylation, are known to regulate the activity of numerous protein kinases.[18,19] Thus, we performed liquid chromatography-tandem mass spectrometry (LC-MS/MS) analysis of CK1α isolated from cells treated with or without Wnt3a to identify potential Wnt-dependent changes in CK1α phosphorylation (Figure 1C). Two Wnt-induced phosphorylation sites were identified on CK1α. The first phosphorylation site was detected on the ^{2}ASSSGSKAEFIVGGK^{16} peptide, with S3 assigned as the phosphorylation site with the highest localization probability (Figures 1D and S2A). The second phosphorylation site was identified on T321 (Figures 1D and S2B). We expressed epitope-tagged *CK1α* constructs encoding wild type (WT) and the two phosphorylation site mutants (HA-CK1α S3A and HA-CK1α T321A) in 293T cells. The epitope-tagged CK1α proteins were subsequently immunoprecipitated and their protein kinase activities measured using recombinant β-catenin as the substrate. HA-CK1α T321A exhibited significantly elevated protein kinase activity relative to HA-CK1α WT and HA-CK1α S3A (Figures 1E and 1F). Together, these results show that Wnt stimulation induces CK1α phosphorylation at T321, which attenuates CK1α protein kinase activity.

Wnt stimulation induces CK1α autophosphorylation on T321

CK1α T321 was previously reported to be an autophosphorylation site in zebrafish CK1α.[20] We therefore performed an *in vitro* kinase assay using purified recombinant human CK1α proteins (WT or CK1α T321A) (Figure S2A) to determine whether the Wnt-dependent phosphorylation of human CK1α T321 we observed in 293T cells is due to autophosphorylation. Human CK1α T321A exhibited significantly reduced autophosphorylation relative to CK1α WT (Figure S3A), consistent with T321 being the major autophosphorylation site in human CK1α. In addition, human CK1α T321A showed increased kinase activity when phosphorylating α-casein *in vitro* (Figure S3B), indicating that CK1α autophosphorylation inhibits CK1α protein kinase activity. We next overexpressed HA-CK1α WT or a kinase-inactive mutant (HA-CK1α K46A) and evaluated T321 phosphorylation in response to Wnt treatment. HA-CK1α K46A showed significantly reduced T321 phosphorylation in response to Wnt3a treatment relative to HA-CK1α WT (Figure 1G). These results suggest that Wnt-induced phosphorylation of CK1α T321 results from Wnt-regulated CK1α autophosphorylation.

Wnt signaling induces the dissociation of CK1α from PP2A

Phospho-regulation of proteins is a highly dynamic process enhanced by protein kinases and reduced by PPs.[18,21] Several serine/threonine PPs, including PP1 and PP2A, are reported to modulate Wnt signaling by regulating the dephosphorylation of various pathway components.[22,23] Thus, we hypothesized that a PP might regulate CK1α autophosphorylation. Our CK1α LC-MS/MS results (see Figure 1C) identified a number of CK1α-associated PPs (Figure 2A), including the PPP2R1A scaffold, the PPP2R2A (B55α) regulatory subunit, and the PPP2CA and PPP2CB catalytic subunits of PP2A (Figure 2A). These PPs are enriched in the CK1α interactome at levels higher than known CK1α interactors, including β-catenin and GSK3. Importantly, these LC-MS/MS results also showed reduced binding of PPP2CA/PPP2CB to CK1α in Wnt-treated cells (Figure 2A, red box). Additionally, our previous global phosphoproteomic analysis showed that the inhibition of PP2A-B55 holoenzymes resulted in increased phosphorylation of CK1α T321[24] and that the PP2A-B55 holoenzyme preferentially dephosphorylated proline-directed threonine phosphorylation sites such as CK1α T321 (AQpTPTG)[24–26] (Figures S4A and S4B). Thus, we speculated that this Wnt-induced dissociation of PPP2CA/PPP2CB from CK1α might result in increased CK1α autophosphorylation due to reduced phosphatase activity at the T321 site. Consistent with this notion, we found that *PPP2CA* knockdown attenuated Wnt-mediated CK1α autophosphorylation at T321, whereas the knockdown of *PPP2CB* or a scrambled control gene (*CTRL*) did not (Figures 2B and S4C). These results also showed that co-immunoprecipitation of PPP2CA and CK1α is reduced following Wnt stimulation (Figure 2B), validating our LC-MS/MS data. We further investigated the interaction of PPP2CA with CK1α using an *in situ* proximity ligation assay (PLA) (Figures 2C and 2D), in which the close proximity of two target proteins results in a fluorescent signal.[27] This assay highlighted a strong interaction between PPP2CA and CK1α, which was significantly decreased upon Wnt treatment. Moreover, the knockdown of PPP2CA significantly reduced CK1α kinase activity (Figure 2E). Together, these results suggest that Wnt stimulation controls CK1α autophosphorylation by regulating its association with PPP2CA.

Wnt stimulation alters the binding dynamics of PPP2CA/CK1α/AXIN1 in the destruction complex

PP2A is known to modulate Wnt signaling via regulation of the destruction complex and the T cell factor (TCF) transcription factor complex.[28,29] Thus, to determine which of these macromolecular complexes is involved in Wnt-dependent CK1α autophosphorylation, we examined the subcellular compartment in which CK1α autophosphorylation is enriched. We noted that CK1α showed a time-dependent increase of T321 phosphorylation in the cytoplasm relative to the nucleus (Figure S5A), consistent with Wnt-driven CK1α autophosphorylation occurring in the destruction complex. We next knocked down the expression of *AXIN1*, which encodes the scaffold protein of the destruction complex. Loss of *AXIN1* significantly attenuated the association of CK1α with PPP2CA (Figures 3A–3C). Moreover, in the presence of a small-molecule AXIN stabilizer, XAV-939,[30] the Wnt-induced dissociation of PPP2CA/CK1α was no longer observed (Figures 3D and 3E). These results suggest that AXIN1 is critical for the PPP2CA-CK1α interaction. Using an *in situ* PLA, we also observed that the binding of PPP2CA to AXIN1 was significantly

CellPress
OPEN ACCESS

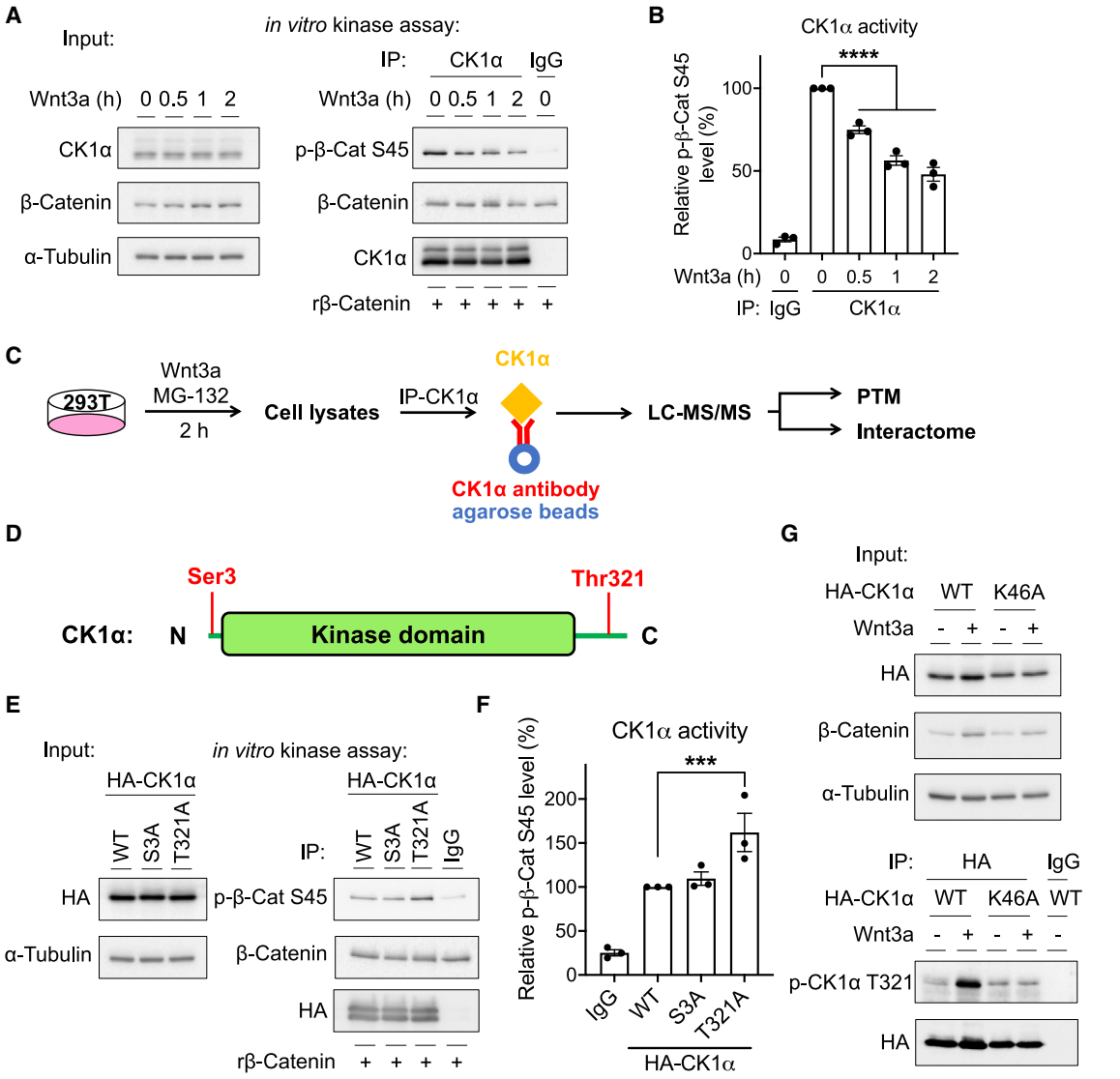

Figure 1. Wnt signaling induces the autophosphorylation and consequent inactivation of CK1α

(A and B) HEK293T cells were treated with Wnt3a ligand for the indicated time periods. CK1α or immunoglobulin (Ig)G (control) immunoprecipitated from lysates of these cells were used for protein kinase reactions in the presence of ATP and recombinant β-catenin. After incubation at 30°C for 30 min, the reactions were stopped by the addition of the Laemmli sample buffer and used for immunoblotting. Representative immunoblots are shown in (A), and the quantification of three such experiments (mean ± SEM) is shown in (B). Asterisks indicate statistical significance (****$p < 0.0001$).

(C) A schematic of the LC-MS/MS experiment used to determine CK1α post-translational modifications (PTMs) and interacting proteins from HEK293T cells, treated with or without Wnt3a.

(D) A schematic showing LC-MS/MS results that identified two Wnt-responsive phosphorylation sites in CK1α: S3 and T321. Phosphorylated residues are highlighted in red.

(E and F) HEK293T cells were transfected with plasmids encoding HA-tagged CK1α wild type (WT) or CK1α phospho-mutants S3A or T321A. Forty-eight hours later, HA-tagged CK1α or an IgG control was immunoprecipitated from the lysates of cells and used for kinase reactions in the presence of ATP and recombinant β-catenin. After incubation at 30°C for 30 min, the reactions were stopped by the addition of the Laemmli sample buffer and used for immunoblotting. Representative immunoblots are shown in (E), and the quantification of the p-β-catenin S45 level normalized to that of HA-CK1α in three such experiments (mean ± SEM) is shown in (F). The asterisk indicates statistical significance (*$p < 0.05$).

(G) HEK293T cells were transfected with plasmids encoding HA-tagged CK1α WT or the CK1α kinase-inactive mutant K46A, followed by Wnt3a treatment for 4 h in the presence of the proteasome inhibitor, MG-132. HA-tagged CK1α or IgG control was immunoprecipitated from cell lysates, followed by immunoblotting. Representative immunoblots are shown ($n = 3$).

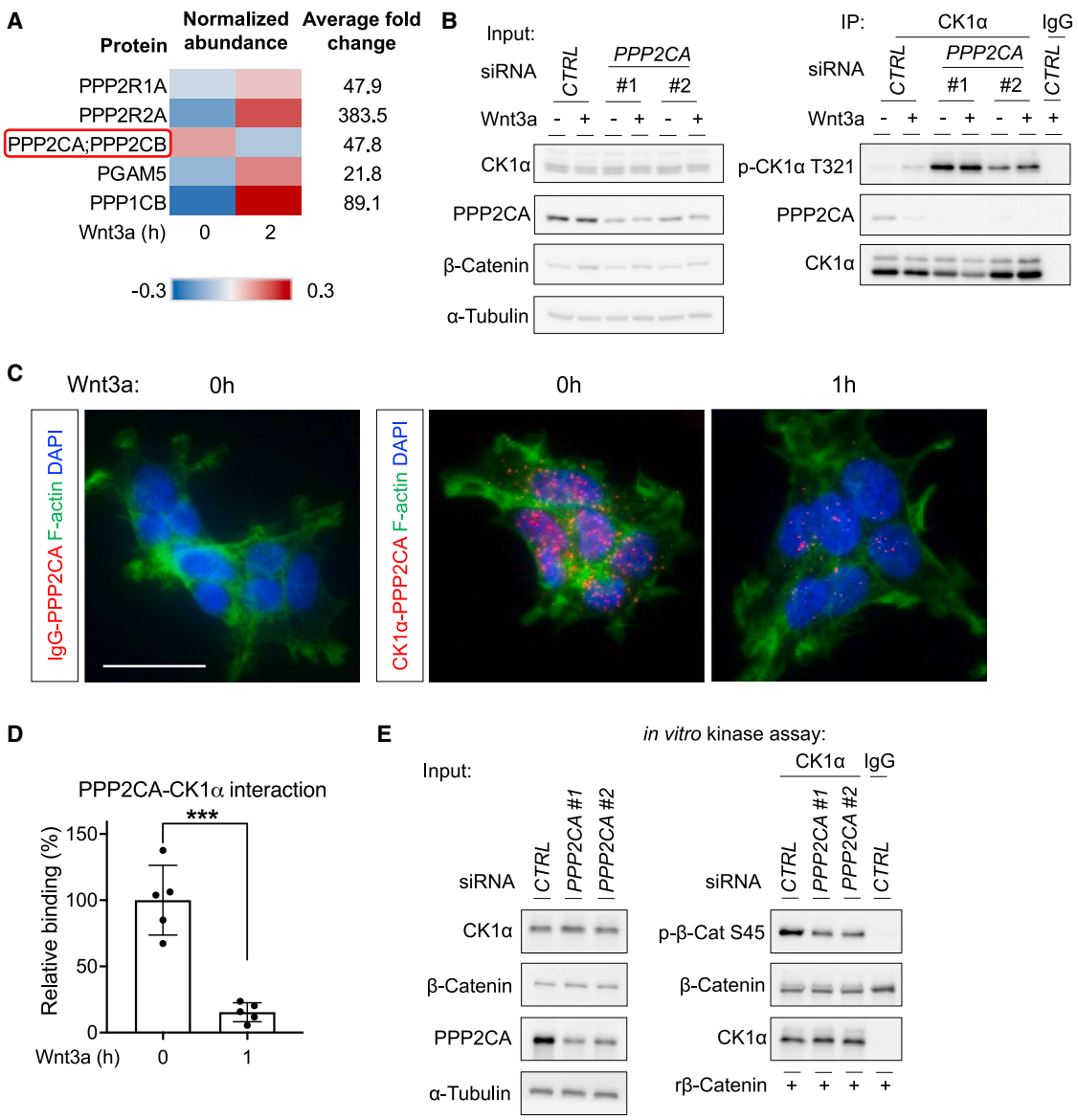

Figure 2. Wnt-dependent CK1α autophosphorylation occurs via dissociation from PPP2CA

(A) A heatmap showing the interaction between CK1α and its five most abundant serine/threonine protein phosphatase components, in the absence or presence of Wnt3a, using the LC-MS/MS experimental approach described in Figure 1C. PPP2CA and/or PPP2CB (red box) showed decreased binding to CK1α in response to Wnt activation. The average fold change shows the enrichment of protein phosphatase components in CK1α immunoprecipitates versus IgG control immunoprecipitates.

(B) HEK293T cells were transfected with small interfering RNAs (siRNAs) for a non-targeting control gene (*CTRL*) or *PPP2CA* (#1 or #2) for 48 h, followed by treatment of Wnt3a and MG-132 for 2 h. CK1α or IgG control was immunoprecipitated from these cell lysates, followed by immunoblotting. Representative immunoblots are shown ($n = 3$).

(C and D) HEK293T cells were treated with Wnt3A for the indicated time periods and used in an *in situ* PLA to quantify the interactions between PPP2CA and CK1α. Interactions are indicated in red, F-actin staining in green, and nuclear staining in blue (DAPI). Representative microscopy images are shown in (C) (scale bar: 25 μm). The quantification of interaction signals in five random fields (mean ± SD) is shown in (D). Asterisks indicate statistical significance (***$p < 0.001$).

(E) HEK293T cells were transfected with siRNAs for a non-targeting control gene (*CTRL*) or *PPP2CA* (#1 or #2) for 72 h. CK1α or IgG (control) immunoprecipitates from the lysates were used for protein kinase reactions in the presence of ATP and recombinant β-catenin. After incubation at 30°C for 30 min, the reactions were stopped by the addition of the Laemmli sample buffer and then used for immunoblotting. Representative immunoblots are shown ($n = 3$).

enhanced in Wnt-treated cells (Figures 3F and 3G), in contrast to the Wnt-induced disassociation of PPP2CA from CK1α (Figures 2C, 2D, and 3F). These results indicate that Wnt stimulation inhibits the interaction between PPP2CA and CK1α but promotes the interaction between PPP2CA and AXIN1 within the β-catenin destruction complex.

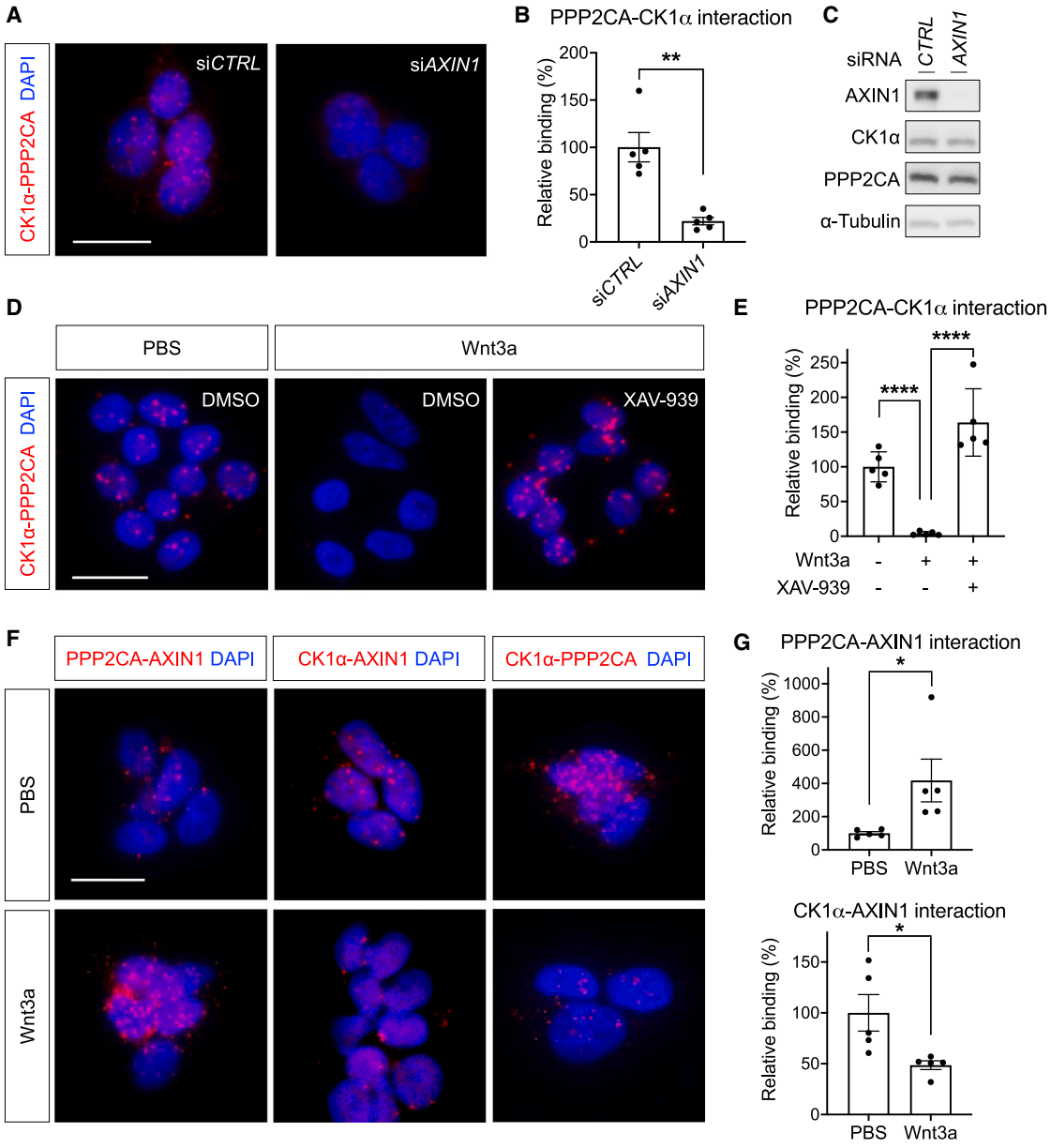

Figure 3. Wnt-dependent, PPP2CA-mediated CK1α autophosphorylation requires AXIN, the scaffold protein of the β-catenin destruction complex

(A–C) HEK293T cells were transfected with siRNA for a non-targeting control gene (*CTRL*) or pooled siRNAs for *AXIN1* for 48 h and then used in an *in situ* PLA to quantify the interactions between PPP2CA and CK1α (A and B) or directly lysed for immunoblotting (C). Representative microscopy images (A) (scale bar: 25 μm) and immunoblots (C) are shown. The quantification of interaction signals in five random fields (mean ± SD) is shown in (B). Asterisks indicate statistical significance (**$p < 0.01$).

(D and E) HEK293T cells were treated with PBS or Wnt3a in the presence or absence of the Axin stabilizer, XAV-939 (10 μM), for 1 h. Cells were then used in an *in situ* PLA to determine the interaction between PPP2CA and CK1α in the absence or presence of Axin stabilization. Interactions are indicated in red and nuclear staining with DAPI in blue. Representative microscopy images are shown in (D) (scale bar: 25 μm). The quantification of interaction signals in five random fields (mean ± SD) is shown in (E). Asterisks indicate statistical significance (****$p < 0.0001$).

(F and G) HEK293T cells were treated with PBS or Wnt3a for 1 h. An *in situ* PLA was then performed to determine the interaction between PPP2CA, CK1α, and AXIN1. Interactions are indicated in red and nuclear staining with DAPI in blue. Representative microscopy images are shown in (F) (scale bar: 25 μm). The quantification of interaction signals in five random fields (mean ± SD) is shown in (G). Asterisk indicates statistical significance (*$p < 0.05$).

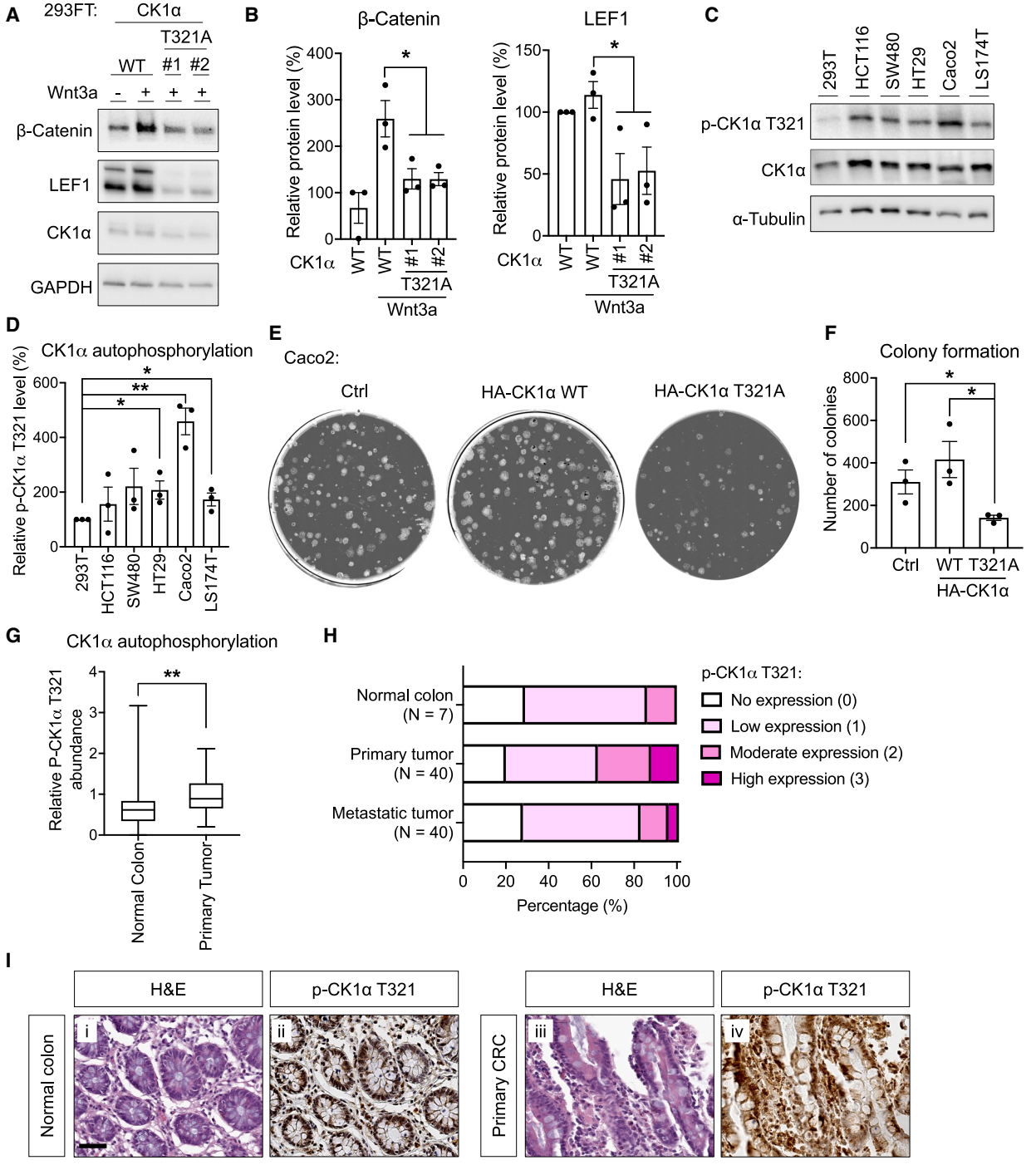

Figure 4. Phosphorylated CK1α-T321 enriches in a subset of CRC

(A and B) Wild-type or CK1α-T321A knockin HEK293FT cells were treated with PBS or Wnt3a (100 ng/mL) for 2 h. Lysates from cells were used for immunoblotting. Representative blots are shown in (A) and the quantification of levels of Wnt activation biomarkers (mean ± SEM, $n = 3$) in (B). The asterisk indicates statistical significance ($^*p < 0.05$).

(C and D) Lysates from HEK293T and five Wnt activity-driven CRC cell lines were used for immunoblotting. Representative blots are shown in (C) and the quantification of autophosphorylated CK1α levels (mean ± SEM, $n = 3$) in (D). Asterisks indicate statistical significance ($^*p < 0.05$ and $^{**}p < 0.01$).

(E and F) The CRC cell line Caco2 was transfected with plasmids encoding HA-tagged CK1α WT or the CK1α mutant lacking the autophosphorylation site (T321A) for 72 h. Transfected cells were then seeded at 1,000 cells/well and grown for 10 days, followed by crystal violet staining of cell colonies. Representative bright-field images are shown in (E) and the quantification of colony number (mean ± SEM, $n = 3$) in (F). The asterisk indicates statistical significance ($^*p < 0.05$).

(legend continued on next page)

Phosphorylated CK1α T321 is enriched in a subset of CRCs

As CK1α is a crucial negative regulator of Wnt signaling, we generated two clonal HEK293FT cell lines with the CK1α T321A mutation knocked in (Figure S6) in order to probe the role of CK1α autoinhibition in Wnt pathway activation. We noted that when two such clonal cell lines were stimulated with Wnt3a, the levels of Wnt activation biomarkers, including β-catenin and lymphoid enhancer-binding factor 1 (LEF1), were significantly decreased compared to similarly treated WT HEK293FT (Figures 4A and 4B). This finding suggests that CK1α autophosphorylation, which inhibits CK1α activity, can enhance Wnt signal transduction.

To examine the potential role of autophosphorylated CK1α, which would be relatively inactive, in enhancing Wnt activity in cancer, we examined CK1α autophosphorylation in multiple human CRC cell lines. Three out of five CRC lines exhibited greater levels of autophosphorylated CK1α, including Caco2, HT29, and LS174T (Figures 4C and 4D). We ectopically expressed an *HA-CK1α* construct lacking the autophosphorylation site (T321A) in two of the CRC cell lines, Caco2 and HT29, and noted that its overexpression attenuated the ability of these CRC cells to grow in a clonogenic assay (Figures 4E, 4F, S7A, and S7B). These results indicate that CK1α autophosphorylation may be important for the propagation of a subset of CRC cell lines. To further investigate the role of CK1α autophosphorylation in CRCs, we analyzed proteomic and phosphoproteomic data generated by the Clinical Proteomic Tumor Analysis Consortium (CPTAC) and found that the abundance of p-CK1α peptide is higher in primary CRC tumor (n = 40) compared to normal colon (n = 26) (Figure 4G). Moreover, we probed a tissue microarray containing primary colorectal tumors, metastatic colorectal tumors, and normal colon samples using immunohistochemistry (IHC). Most normal colon samples exhibit low levels of autophosphorylated CK1α (57%; Figures 4H, 4Ii, 4Iii, and S7C; Table 1). However, high levels of autophosphorylated CK1α were observed in a subset of primary and metastatic CRC samples (13% and 5%, respectively), especially in primary rectal tumors, which have a greater risk of recurrence (Figures 4H, 4Iiii, 4Iiv, and S7C; Table 1). These results suggest that CK1α autophosphorylation and its consequent inactivation may play a role in a subset of CRCs driven by Wnt activity.

DISCUSSION

Our work fills an important gap in the understanding of how CK1α is regulated by Wnt signaling. In the prevailing model, CK1α functions as a constitutively active kinase in Wnt signaling. In contrast, we now show that CK1α protein kinase activity is attenuated in response to Wnt stimulation, extending prior findings from other groups.[7,17] Furthermore, we now propose a model in which CK1α is kept in an active state via its association with PP2A, which dynamically removes the inhibitory autophosphorylation of CK1α at T321. Upon Wnt activation, the association of the PP2A catalytic subunit with CK1α is decreased, allowing the accumulation of autophosphorylated, inactive CK1α. This model also posits that the remodeling of the destruction complex in response to Wnt stimulation results in the autophosphorylation and inactivation of CK1α, with a resultant decrease in β-catenin phosphorylation and degradation. Furthermore, we suggest that this mechanism of CK1α autoinhibition and its resultant increase in Wnt activity may be relevant in a subset of CRCs.

Two CK1 isoforms, δ and ε, have each been reported to autophosphorylate their C-terminal extension, distal to their conserved protein kinase domain.[13,16] It was originally suggested that CK1α lacked this ability, as its C-terminal extension is minimal. Our results show that Wnt-responsive autophosphorylation of human CK1α occurs at T321, a C-terminal site that is highly conserved in other vertebrates. Despite the high sequence similarity among CK1 family members, CK1α T321 is not conserved with the autophosphorylation sites of CK1δ and ε, suggesting the presence of different autophosphorylation mechanisms within the CK1 family. The function of CK1δ/ε has been shown to be modulated by the B56 regulatory subunit of PP2A in Wnt signaling[31]; however, we did not observe an interaction between CK1α and PP2A B56 in our LC-MS/MS analysis. The most abundant PP2A holoenzyme that associates with CK1α contains the B55α subunit (PPP2R2A; Figure 2A). Thus, it is possible that PPP2R2A also participates in the regulation of CK1α during Wnt signaling.

Various subunits of PP2A associate with AXIN1 to regulate Wnt signaling.[29,32] However, the dynamics of this PP2A-AXIN1 complex is poorly understood. We showed that PPP2CA exhibits increased interaction with AXIN1 in response to Wnt pathway activation, which could result in its dissociation with CK1α. Notably, when AXIN1 is stabilized in the presence of Wnt using a tankyrase inhibitor, the PPP2CA-CK1α association is readily detected. Thus, we speculate that AXIN1 serves as a scaffold of the PPP2CA-CK1α interaction, with Wnt signaling regulating the dynamics of this PPP2CA-CK1α-AXIN1 complex to modulate the inactivation of CK1α. Tankyrase small-molecule inhibitors (TANKis) have shown great efficacy in attenuating the growth of Wnt-driven tumors, and several are currently under clinical evaluation (ClinicalTrials.gov: NCT03562832L, NCT05475184, and NCT05257993). Our results suggest that TANKis work in part by increasing the levels of AXIN to mediate the reassociation of PPP2CA with CK1α, thus highlighting a potential strategy to inhibit Wnt-driven tumorigenesis. Furthermore, as CK1α is a ubiquitous protein kinase that regulates a large number of biological events in addition to Wnt signaling, we speculate that CK1α autophosphorylation, and subsequent inactivation, might also be utilized in other

(G) Peptide abundance of p-CK1α T321 in normal colon (n = 26) and primary CRC tumor (n = 40) was mined from the proteomic and phosphoproteomic data generated by CPTAC. To quantitate autophosphorylated CK1α, the abundance of p-CK1α T321 peptides was normalized to that of total CK1α protein. Asterisks indicate statistical significance (**$p < 0.01$).

(H and I) A tissue microarray containing samples from normal colon, primary colorectal cancer, or metastatic colorectal cancer (N = 60 from 49 patients) was used to determine the levels of autophosphorylated CK1α by immunohistochemistry. Representative images of H&E and autophosphorylated CK1α staining are shown in (I) (scale bar: 50 μm). The quantification of CK1α autophosphorylation levels across the tissue microarray are shown in (H).

Table 1. Phosphorylated CK1α T321 levels in CRC patient samples

Tissue	Diagnosis	Score			
		No expression (0)	Low (1)	Moderate (2)	High (3)
Normal					
Colon	normal	2/7	4/7	1/7	0/7
Primary tumor					
rectum	adenocarcinoma	2/12	3/12	3/12	4/12
colon	adenocarcinoma	6/28	14/28	7/28	1/28
Metastasis					
colon	metastatic adenocarcinoma	3/13	7/13	2/13	1/13
liver	metastatic adenocarcinoma	6/21	11/21	3/21	1/21
uterus	metastatic adenocarcinoma	0/2	2/2	0/2	0/2
omentum	metastatic adenocarcinoma	0/2	2/2	0/2	0/2
muscle	metastatic adenocarcinoma	2/2	0/2	0/2	0/2

signaling pathways—underscoring the biological significance of our findings.

Limitations of the study

The assays used in our study to determine protein-protein interactions, including both co-immunoprecipitation and *in situ* PLA, are largely dependent on the antibodies utilized and provide limited information on the dynamics of a multiprotein complex. In addition, although results from experiments using CK1α T321A support the stated conclusion, we have observed more ambiguous results when using the putative phospho-mimetic mutant CK1α T321D, and such data were not included in this manuscript.

RESOURCE AVAILABILITY

Lead contact

Further information and request for resources and materials should be directed to and will be made available by the lead contact, David J. Robbins (dr956@georgetown.edu).

Materials availability

Reagents generated in this study will be made available from the lead contact.

Data and code availability

- The MS proteomics data have been deposited into ProteomeXchange consortium and MassIVE repository and are publicly available as of the date of publication. The accession numbers are listed in the key resources table.
- No original code is generated in this study.
- Any additional information required will be available from the lead contact upon request.

ACKNOWLEDGMENTS

We thank all members of the Robbins, Lee, Ahmed, and Cobb laboratories for their insightful advice and discussion regarding this work. This work was supported by Lombardi Comprehensive Cancer Center developmental funds; the following NIH grants: R01CA219189, R01CA244188, R01CA281002, R35GM122516, R35GM136233, and R50CA221838; the Histopathology and Tissue Shared Resource of the Georgetown Lombardi Comprehensive Cancer Center (P30-CA051008); and the Edwin H. Richard and Elisabeth Richard von Matsch Endowed Chair in Experimental Therapeutics and JPMorgan Private Bank to D.J.R.

AUTHOR CONTRIBUTIONS

Conceptualization, C.S., M.H.C., Y.A., E.L., and D.J.R.; experimental design, C.S., W.L., S.B.M., L.S., F.Y., C.C., H.-Y.T., C.A., C.I., and D.J.R.; investigation, C.S., W.L., S.B.M., A.B., S.M.A., L.S., F.Y., T.M.R., A.N., and H.-Y.T.; data analysis, C.S., W.L., S.B.M., A.B., S.M.A., L.S., D.T.W., F.Y., H.-Y.T., and B.T.H.; writing – original draft, C.S. and D.J.R.; writing – editing, W.L., S.B.M., A.B., S.M.A., L.S., D.T.W., F.Y., T.M.R., N.B., M.H.C., Y.A., and E.L.; visualization, C.S., W.L., S.B.M., and L.S.; supervision, D.J.R.; funding acquisition, Y.A., E.L., A.K., and D.J.R.

DECLARATION OF INTERESTS

D.J.R. and E.L. are founders of StemSynergy Therapeutics, Inc., a company commercializing small-molecule signaling inhibitors, including Wnt inhibitors.

STAR★METHODS

Detailed methods are provided in the online version of this paper and include the following:

- KEY RESOURCES TABLE
- EXPERIMENTAL MODEL AND STUDY PARTICIPANT DETAILS
  - Subject details
- METHOD DETAILS
  - Cellular assays
  - Immunoprecipitation
  - *In vitro* kinase assay
  - *In situ* proximity ligation assay
  - Mass spectrometry
  - Immunohistochemistry
  - Generation of CK1α T321A knock-in HEK293FT cells
- QUANTIFICATION AND STATISTICAL ANALYSIS

SUPPLEMENTAL INFORMATION

Supplemental information can be found online at https://doi.org/10.1016/j.celrep.2025.115274.

Received: August 10, 2023
Revised: August 30, 2024
Accepted: January 16, 2025
Published: February 6, 2025

REFERENCES

1. Bugter, J.M., Fenderico, N., and Maurice, M.M. (2021). Mutations and mechanisms of WNT pathway tumour suppressors in cancer. Nat. Rev. Cancer *21*, 5–21. https://doi.org/10.1038/s41568-020-00307-z.
2. Rim, E.Y., Clevers, H., and Nusse, R. (2022). The Wnt Pathway: From Signaling Mechanisms to Synthetic Modulators. Annu. Rev. Biochem. *91*, 571–598. https://doi.org/10.1146/annurev-biochem-040320-103615.
3. Stamos, J.L., and Weis, W.I. (2013). The beta-catenin destruction complex. Cold Spring Harbor Perspect. Biol. *5*, a007898. https://doi.org/10.1101/cshperspect.a007898.
4. Orford, K., Crockett, C., Jensen, J.P., Weissman, A.M., and Byers, S.W. (1997). Serine phosphorylation-regulated ubiquitination and degradation of beta-catenin. J. Biol. Chem. *272*, 24735–24738. https://doi.org/10.1074/jbc.272.40.24735.
5. Munemitsu, S., Albert, I., Souza, B., Rubinfeld, B., and Polakis, P. (1995). Regulation of intracellular beta-catenin levels by the adenomatous polyposis coli (APC) tumor-suppressor protein. Proc. Natl. Acad. Sci. USA *92*, 3046–3050. https://doi.org/10.1073/pnas.92.7.3046.
6. Hart, M.J., de los Santos, R., Albert, I.N., Rubinfeld, B., and Polakis, P. (1998). Downregulation of beta-catenin by human Axin and its association with the APC tumor suppressor, beta-catenin and GSK3 beta. Curr. Biol. *8*, 573–581. https://doi.org/10.1016/s0960-9822(98)70226-x.
7. Amit, S., Hatzubai, A., Birman, Y., Andersen, J.S., Ben-Shushan, E., Mann, M., Ben-Neriah, Y., and Alkalay, I. (2002). Axin-mediated CKI phosphorylation of beta-catenin at Ser 45: a molecular switch for the Wnt pathway. Genes Dev. *16*, 1066–1076. https://doi.org/10.1101/gad.230302.
8. Liu, C., Li, Y., Semenov, M., Han, C., Baeg, G.H., Tan, Y., Zhang, Z., Lin, X., and He, X. (2002). Control of beta-catenin phosphorylation/degradation by a dual-kinase mechanism. Cell *108*, 837–847. https://doi.org/10.1016/s0092-8674(02)00685-2.
9. Shen, C., Nayak, A., Melendez, R.A., Wynn, D.T., Jackson, J., Lee, E., Ahmed, Y., and Robbins, D.J. (2020). Casein kinase 1α as a regulator of wnt-driven cancer. Int. J. Mol. Sci. *21*, 5940. https://doi.org/10.3390/ijms21165940.
10. Thorne, C.A., Hanson, A.J., Schneider, J., Tahinci, E., Orton, D., Cselenyi, C.S., Jernigan, K.K., Meyers, K.C., Hang, B.I., Waterson, A.G., et al. (2010). Small-molecule inhibition of Wnt signaling through activation of casein kinase 1α. Nat. Chem. Biol. *6*, 829–836. https://doi.org/10.1038/nchembio.453.
11. Li, B., Orton, D., Neitzel, L.R., Astudillo, L., Shen, C., Long, J., Chen, X., Kirkbride, K.C., Doundoulakis, T., Guerra, M.L., et al. (2017). Differential abundance of CK1alpha provides selectivity for pharmacological CK1alpha activators to target WNT-dependent tumors. Sci. Signal. *10*, eaak9916. https://doi.org/10.1126/scisignal.aak9916.
12. Knippschild, U., Gocht, A., Wolff, S., Huber, N., Löhler, J., and Stöter, M. (2005). The casein kinase 1 family: participation in multiple cellular processes in eukaryotes. Cell. Signal. *17*, 675–689. https://doi.org/10.1016/j.cellsig.2004.12.011.
13. Cegielska, A., Gietzen, K.F., Rivers, A., and Virshup, D.M. (1998). Autoinhibition of casein kinase I epsilon (CKI epsilon) is relieved by protein phosphatases and limited proteolysis. J. Biol. Chem. *273*, 1357–1364. https://doi.org/10.1074/jbc.273.3.1357.
14. Swiatek, W., Tsai, I.C., Klimowski, L., Pepler, A., Barnette, J., Yost, H.J., and Virshup, D.M. (2004). Regulation of casein kinase I epsilon activity by Wnt signaling. J. Biol. Chem. *279*, 13011–13017. https://doi.org/10.1074/jbc.M304682200.
15. Cullati, S.N., Chaikuad, A., Chen, J.S., Gebel, J., Tesmer, L., Zhubi, R., Navarrete-Perea, J., Guillen, R.X., Gygi, S.P., Hummer, G., et al. (2022). Kinase domain autophosphorylation rewires the activity and substrate specificity of CK1 enzymes. Mol. Cell *82*, 2006–2020.e8. https://doi.org/10.1016/j.molcel.2022.03.005.
16. Graves, P.R., and Roach, P.J. (1995). Role of COOH-terminal phosphorylation in the regulation of casein kinase I delta. J. Biol. Chem. *270*, 21689–21694. https://doi.org/10.1074/jbc.270.37.21689.
17. Hernández, A.R., Klein, A.M., and Kirschner, M.W. (2012). Kinetic responses of beta-catenin specify the sites of Wnt control. Science *338*, 1337–1340. https://doi.org/10.1126/science.1228734.
18. Cohen, P. (2002). The origins of protein phosphorylation. Nat. Cell Biol. *4*, E127–E130. https://doi.org/10.1038/ncb0502-e127.
19. Millar, A.H., Heazlewood, J.L., Giglione, C., Holdsworth, M.J., Bachmair, A., and Schulze, W.X. (2019). The Scope, Functions, and Dynamics of Posttranslational Protein Modifications. Annu. Rev. Plant Biol. *70*, 119–151. https://doi.org/10.1146/annurev-arplant-050718-100211.
20. Budini, M., Jacob, G., Jedlicki, A., Pérez, C., Allende, C.C., and Allende, J.E. (2009). Autophosphorylation of carboxy-terminal residues inhibits the activity of protein kinase CK1alpha. J. Cell. Biochem. *106*, 399–408. https://doi.org/10.1002/jcb.22019.
21. Barford, D., Das, A.K., and Egloff, M.P. (1998). The structure and mechanism of protein phosphatases: insights into catalysis and regulation. Annu. Rev. Biophys. Biomol. Struct. *27*, 133–164. https://doi.org/10.1146/annurev.biophys.27.1.133.
22. Luo, W., Peterson, A., Garcia, B.A., Coombs, G., Kofahl, B., Heinrich, R., Shabanowitz, J., Hunt, D.F., Yost, H.J., and Virshup, D.M. (2007). Protein phosphatase 1 regulates assembly and function of the beta-catenin degradation complex. EMBO J. *26*, 1511–1521. https://doi.org/10.1038/sj.emboj.7601607.
23. Thompson, J.J., and Williams, C.S. (2018). Protein phosphatase 2A in the regulation of Wnt signaling. Genes *9*, 121. https://doi.org/10.3390/genes9030121.
24. Kruse, T., Gnosa, S.P., Nasa, I., Garvanska, D.H., Hein, J.B., Nguyen, H., Samsøe-Petersen, J., Lopez-Mendez, B., Hertz, E.P.T., Schwarz, J., et al. (2020). Mechanisms of site-specific dephosphorylation and kinase opposition imposed by PP2A regulatory subunits. EMBO J. *39*, e103695. https://doi.org/10.15252/embj.2019103695.
25. Nguyen, H., and Kettenbach, A.N. (2023). Substrate and phosphorylation site selection by phosphoprotein phosphatases. Trends Biochem. Sci. *48*, 713–725. https://doi.org/10.1016/j.tibs.2023.04.004.
26. Hein, J.B., Nguyen, H.T., Garvanska, D.H., Nasa, I., Feng, Y., Mendez, B.L., Davey, N., Kettenbach, A.N., Fordyce, P.M., and Nilsson, J. (2023). Global substrate identification and high throughput in vitro dephosphorylation reactions uncover PP1 and PP2A-B55 specificity principles. Preprint at bioRxiv. https://doi.org/10.1101/2023.05.14.540683.
27. Bagchi, S., Fredriksson, R., and Wallén-Mackenzie, Å. (2015). In Situ Proximity Ligation Assay (PLA). Methods Mol. Biol. *1318*, 149–159. https://doi.org/10.1007/978-1-4939-2742-5_15.
28. Ratcliffe, M.J., Itoh, K., and Sokol, S.Y. (2000). A positive role for the PP2A catalytic subunit in Wnt signal transduction. J. Biol. Chem. *275*, 35680–35683. https://doi.org/10.1074/jbc.C000639200.
29. Li, X., Yost, H.J., Virshup, D.M., and Seeling, J.M. (2001). Protein phosphatase 2A and its B56 regulatory subunit inhibit Wnt signaling in Xenopus. EMBO J. *20*, 4122–4131. https://doi.org/10.1093/emboj/20.15.4122.
30. Huang, S.M.A., Mishina, Y.M., Liu, S., Cheung, A., Stegmeier, F., Michaud, G.A., Charlat, O., Wiellette, E., Zhang, Y., Wiessner, S., et al. (2009). Tankyrase inhibition stabilizes axin and antagonizes Wnt signalling. Nature *461*, 614–620. https://doi.org/10.1038/nature08356.
31. Gao, Z.H., Seeling, J.M., Hill, V., Yochum, A., and Virshup, D.M. (2002). Casein kinase I phosphorylates and destabilizes the beta-catenin degradation complex. Proc. Natl. Acad. Sci. USA *99*, 1182–1187. https://doi.org/10.1073/pnas.032468199.
32. Yamamoto, H., Hinoi, T., Michiue, T., Fukui, A., Usui, H., Janssens, V., Van Hoof, C., Goris, J., Asashima, M., and Kikuchi, A. (2001). Inhibition

of the Wnt signaling pathway by the PR61 subunit of protein phosphatase 2A. J. Biol. Chem. *276*, 26875–26882. https://doi.org/10.1074/jbc.M100443200.

33. Shen, C., Li, B., Astudillo, L., Deutscher, M.P., Cobb, M.H., Capobianco, A.J., Lee, E., and Robbins, D.J. (2019). The CK1alpha Activator Pyrvinium Enhances the Catalytic Efficiency (kcat/Km) of CK1alpha. Biochemistry *58*, 5102–5106. https://doi.org/10.1021/acs.biochem.9b00891.
34. Cox, J., and Mann, M. (2008). MaxQuant enables high peptide identification rates, individualized p.p.b.-range mass accuracies and proteome-wide protein quantification. Nat. Biotechnol. *26*, 1367–1372. https://doi.org/10.1038/nbt.1511.

STAR★METHODS

KEY RESOURCES TABLE

REAGENT or RESOURCE	SOURCE	IDENTIFIER
Antibodies		
Anti CK1α	Abcam	Cat# ab108296 or 206652; RRID: AB_10864123 or 2925161
Anti CK1α	Bethyl Laboratories	Cat# A301-991A; RRID: AB_1576501
Anti p-β-Catenin S45	Cell Signaling Technology	Cat# 9564; RRID: AB_331150
Anti β-Catenin	Cell Signaling Technology	Cat# 9562; RRID: AB_331149
Anti α-Tubulin	MilliporeSigma	Cat# T9199
Anti HA-tag	Cell Signaling Technology	Cat# 3724; RRID: AB_1549585
Anti HA-tag agarose	MilliporeSigma	Cat# A2095
Anti p-CK1α T321	Invitrogen	Cat# PA5-36790; RRID: AB_2553736
Anti PPP2CA	BD Biosciences	Cat# 610555; RRID: AB_397909
Anti PPP2CB	Abcam	Cat# ab168371
Anti SP1	Cell Signaling Technology	Cat# 9389; RRID: AB_11220235
Anti Axin1	Cell Signaling Technology	Cat# 2087; RRID: AB_2274550
Anti Axin1	MilliporeSigma	Cat# 05-1579; RRID: AB_11212277
Anti Axin2	Cell Signaling Technology	Cat# 2151; RRID: AB_2062432
Anti LEF1	Abcam	Cat# ab137872; RRID: AB_2892647
HRP-conjugated donkey anti-mouse or anti-rabbit	Jackson ImmunoResearch	Cat# 715-035-150 or 711-035-152
Chemicals, peptides and recombinant proteins		
Recombinant Wnt3a	R&D Systems	Cat# 5036-WN-010
Recombinant Wnt3a	Time Bioscience	Cat# rhW3aH
Recombinant Frizzled8-CRD	R&D Systems	Cat# 6129-FZ
Recombinant human β-Catenin	Sigma	Cat# SRP5172
Recombinant human CK1α WT, T321A	This paper; Genscript	N/A
Dephosphorylated α-Casein	Sigma	Cat# C8032
MG-132	Selleckchem	Cat# S2619
XAV-939	Selleckchem	Cat# S1180
Oligonucleotides		
Smart-pooled siRNA: si*PPP2CA*	Dharmacon	Cat# L-003598-01
Smart-pooled siRNA: si*PPP2CB*	Dharmacon	Cat# L-003599-00
Smart-pooled siRNA: si*AXIN1*	Dharmacon	Cat# L-009625-00
Smart-pooled siRNA: si*AXIN2*	Dharmacon	Cat# L-008809-00
Individual siRNA: si*PPP2CA* #1 or 2	Dharmacon	Cat# J-003598-09 or J-003598-10
Critical commercial assays		
Duolink® *in situ* PLA® probes	Sigma	Cat# DUO92002 or 92004
Duolink® *in situ* detection reagents red	Sigma	Cat# DUO92008
ADP-Glo™ kinase assay	Promega	Cat# V9101
Deposited data		
Mass spectrometry data	This paper	N/A
Mass spec of CK1α phosphorylation sites with Wnt3a 0 or 2 h	ProteomeXchange consortium	PXD056028
Mass spec of CK1α phosphorylation sites with Wnt3a 0 or 2 h	MassIVE repository	MSV000095904

(*Continued on next page*)

Continued

REAGENT or RESOURCE	SOURCE	IDENTIFIER
Experimental models: Cell lines		
HEK293T cells	ATCC	Cat# CRL-3216
HEK293FT cells	Invitrogen	Cat# R70007
CRC cell lines	Tissue Culture Core facility, Georgetown University	N/A
Recombinant DNA		
Plasmids: HA-CK1α WT, S3A, T321A, K46A, S3D, T321D in pcDNA3.1+	This paper; Genscript	N/A
Software and algorithms		
ImageJ	National Institutes of Health	http://imagej.nih.gov
Prism 9	GraphPad Software	http://graphpad.com

EXPERIMENTAL MODEL AND STUDY PARTICIPANT DETAILS

Subject details

Human subject

Non-critical tissue samples were collected under the approval of the IRB (Pro00023460) of Medstar-Georgetown. All participants were provided written informed consent before participation in this study and before accrual of specimens or clinical information. Detailed information of human participants in this study is included in Table S1.

METHOD DETAILS

Cellular assays

All cells were purchased from ATCC or Tissue Culture and Biobanking Shared Resource (Lombardi Comprehensive Cancer Center, Georgetown University) without further authentication. All cells were tested mycoplasma negative prior to investigation. Cells were cultured as per ATCC instructions. Recombinant Wnt3a were reconstituted according to manufacturer's protocol and used at 250 ng/mL in all experiments unless otherwise indicated. Cytoplasmic and nuclear cell fractions were separated using NE-PER Extraction Kit (Thermo fisher). siRNA transfection, 50 nM siRNA, was transfected using Lipofectamine RNAiMax reagent (Invitrogen). Plasmid transfection was performed using Lipofectamine 2000 reagent (Invitrogen).

Immunoprecipitation

Cells treated with Wnt3a or transfected with HA-tagged CK1α plasmids were lysed with Pierce IP lysis buffer (Thermo Fisher) containing a protease and phosphatase inhibitor cocktail (Thermo fisher) on a rocker platform for 10 min at 4°C, followed by centrifugation at 16,000 g for 10 min using a 4°C tabletop centrifuge. CK1α (Abcam ab206652) antibody was pre-conjugated to agarose beads using Aminolink plus immobilization kit (Thermo fisher). HA-conjugated beads were purchased from MilliporeSigma. Cell lysates were incubated with antibody or IgG conjugated beads overnight at 4°C, followed by three 10 min washes with lysis buffer at 4°C. Immunoprecipitated proteins were eluted by boiling in Laemmli buffer supplemented with β-mercaptoethanol and a protease and phosphatase inhibitor cocktail (Thermo fisher) for 5 min and subjected to SDS-PAGE and immunoblotting.

In vitro kinase assay

CK1α immunoprecipitated from cells were diluted in protein kinase buffer[33] in the presence of 50 μM Ultrapure ATP (Promega), with or without 1 μg recombinant β-Catenin to a final volume of 50 μL. Similarly, recombinant CK1α protein (Genscript) was added to 50 μM Ultrapure ATP (Promega), with or without dephosphorylated α-Casein (Sigma) to a final volume of 50 μL in protein kinase buffer. The mixtures were then incubated at 30°C for 30 min. Kinase reactions were stopped on ice or by adding Laemmli sample buffer and kinase activity detected by ADP-Glo assay (Promega) or immunoblotting to detect p-β-Catenin S45 level.

In situ proximity ligation assay

Cells were grown and immobilized on poly-L-lysine coated coverslips (Corning, 354085) overnight and then subjected to indicated treatments. The treated cells were fixed in 4% formaldehyde in PBS for 10 min at room temperature, followed by two washes in PBS containing 3% BSA. The fixed samples were subsequentially permeabilized in 0.5% Triton X-100 in PBS for 20 min at room temperature and washed in PBS for three times, followed by PLA assays using Duolink *In Situ* Kit Mouse/Rabbit (Sigma) as per the manufacturer's instruction. Antibodies (anti CK1α (Bethyl Laboratories), anti PPP2CA (BD Biosciences), anti Axin1 (MilliporeSigma)) were used at 1:200 dilution. Control IgGs (normal mouse IgG (Santa Cruz Biotechnology, sc-2343), and rabbit IgG (MilliporeSigma, 12370)

were used at same concentrations as antibodies. DAPI (Invitrogen, P36935) and F-actin (Invitrogen, R37110) were used as costains and coverslip mounting was done using ProLong Gold Antifade Mountant. Samples were imaged using a fluorescence microscope (Keyence). Images of five independent fields were taken for each sample, and the interaction intensities were measured, as the ratio of the overall red signaling intensity (by ImageJ) to the amount of DAPI stained cells (by Keyence Software).

Mass spectrometry

After excision, gel bands were subjected to TCEP reduction and iodoacetamide alkylation before in-gel trypsin digestion. Samples were then loaded onto a UPLC Symmetry trap column (180 μm i.d. x 2 cm packed with 5 μm C18 resin; Waters) in a Nano-ACQUITY UPLC system (Waters). Reversed phase HPLC was used to separate tryptic peptides with a BEH C18 nanocapillary analytical column (75 μm i.d. x 25 cm, 1.7 μm particle size; Waters) and a 90 min gradient of solvent A (0.1% formic acid in water) and solvent B (0.1% formic acid in acetonitrile). Eluted peptides were analyzed on a Q Exactive HF mass spectrometer (Thermo Fisher Scientific) in positive ion mode scanning m/z from 300 to 1650. 60,000 resolution was used for the full MS scan and the subsequent data-dependent MS/MS scans on the 12 most abundant ions were performed at 15,000. Settings were adjusted such that peptide match was set to preferred and the exclude isotopes option and charge-state screening were enabled. MaxQuant 1.6.17.0[34] was used to identify peptides and phosphorylation sites. MS/MS spectra were searched against the UniProt human protein database (10/10/2019). False discovery rates of 1% at protein, peptide and site levels were used to create consensus identification lists. The phosphorylation site was assigned to the amino acid residue with the highest localization probability.

Immunohistochemistry

The TMA blocks from primary and metastatic CRC were sliced into thin 5μm slices using a microtome (Microm HM340E, Histocom, Zug, Switzerland). A total of 60 surgical tissue cores from 49 patients were included in two TMAs. The TMA sections were stained with Hematoxylin 0.5% (Sigma-Aldrich, St. Louis, MO, USA) and Eosin Y (Sigma-Aldrich, St. Louis, MO, USA). For immunostaining, TMAs were stained with anti Phospho-CK1α T321 antibody (Invitrogen) for the analysis of autophosphorylated CK1α on tumors. After deparaffinization, the samples were blocked with hydrogen peroxide and normal serum (Vector Laboratories, Burlingame, CA, USA). Subsequently, an overnight incubation at 4°C was performed with a diluted antibody of 1:25. A biotinylated secondary antibody was incubated after primary incubation (Vector Laboratories, Burlingame, CA, USA), followed by an ABC reagent incubation (Vector Laboratories, Burlingame, CA, USA). The detection was carried out using DAB substrates (3.32′-diaminobenzidine) from Vector Laboratories, Burlingame, California, USA. In addition to counterstaining with hematoxylin, sections were mounted. An Aperio GT450: High capacity, automated digital slide scanner was used to scan stained TMAs. Images were taken by a Keyence microscope.

Generation of CK1α T321A knock-in HEK293FT cells

CRISPR was used to generate stable point mutation lines in HEK293FT cells. Guide RNAs were selected within 10 base pairs of the residue of interest. A donor plasmid was created containing the donor sequence to introduce the point mutation along with a guide plasmid containing Cas9 and a fluorescent marker. The guide and donor plasmid were transfected into cells using Lipofectamine 3000 (Invitrogen). The cells were allowed to recover for 48 h and then were single cell sorted for the fluorescent tag. The sorted cells were grown for two weeks and then validated as single colonies. Colonies were expanded, followed by genomic DNA extraction using a Qiagen DNeasy kit. The region harboring the point mutation was expanded using primers bordering the mutated residue with around 75 nucleotides on either side. The PCR amplification was completed using Promega PCR Master Mix. These amplified products were cleaned using the Qiagen PCR clean-up kit and then sent for Sanger Sequencing. The lines that were positive for the mutation were used in subsequent experiments.

QUANTIFICATION AND STATISTICAL ANALYSIS

Chemiluminescent signals were quantitated using ImageJ. All experiments were independently repeated at least three times. Quantifications indicate mean ± S.E.M., expect for the PLA results which are shown as mean ± S.D. of five random microscopy fields and *in vitro* kinase assays which are shown as mean ± S.D. of three technical replicates. Statistical significance was determined by an unpaired two-tailed Student's *t*-test except for colony formation assays (paired two-tailed Student's *t*-test) and analysis of CPTAC proteomic and phosphoproteomic data (non-parametric Mann Whitney test) using Prism 9. Asterisks indicate statistical significance (*p values $\leq$ 0.05; **p values $\leq$ 0.01; ***p values $\leq$ 0.001; ****p values $\leq$ 0.0001).